Single Phase Flow Pressure Drop and Heat Transfer in a Rectangular Metallic Micro channel

Amirah M. SAHAR[1], Mehmed R. OZDEMIR[1], Mohamed M. MAHMOUD[1,2*], Jan WISSINK[1], Tassos G. KARAYIANNIS[1]
* Corresponding author: mohamed.mahmoud@brunel.ac.uk
1 School of Engineering and Design, Brunel University, UK
2 Faculty of Engineering, Zagazig University, Egypt

Abstract Numerical simulations were performed using Fluent 14.5 to investigate single-phase flow and conjugate heat transfer in a rectangular microchannel embedded in a heated copper block with a glass plate on top. The hydraulic diameter of the rectangular channel was 0.561 mm and its length was 62 mm. The working fluid used in this investigation was water and the Reynolds number was varied from 100 to 3000. Three models were investigated namely 2D, 3D thin-wall (heated from the bottom and three side heated) and 3D fully conjugate models. The numerical results were validated using experimental data and existing conventional theory. The experimental data were found to be in excellent agreement with the 3D thin-wall models while it were under predicted using the 3D full conjugate and 2D models. These findings demonstrated that the numerical scheme that was employed is able to provide an accurate simulation of flow and heat transfer in a microchannel. Also, the results demonstrated that there is a significant difference between the 3D thin-wall and fully conjugate models.

Keywords: Microchannel, Single phase flow, Heat transfer

1. Introduction

Microchannel heat exchangers have several advantages over macro-scale ones due to their high surface-to-volume ratio and their small overall volume. The large surface-to-volume ratio leads to high rate of heat transfer and, consequently, makes microchannels excellent tools for compact and ultra-compact heat exchangers. Additionally, the growing interest of the industrial community in microdevices and their wide applications especially in cooling high-heat-flux devices such as electronic systems has motivated many researchers to investigate flow phenomena in microchannels. These researchers have focused on understanding the characteristics of heat transfer and fluid flow at micro scale level in order to improve the design and optimize the performance of microchannel heat exchangers.

Single phase microchannel studies started with Tuckerman and Pease`s (1981) pioneering work in which they studied the heat transfer capability of water flowing under laminar conditions through silicon wafer microchannels. Heat flux value of 790 W/cm^2 was achieved while the chip temperature was maintained below 110 °C. Many researchers subsequently proceeded to study characteristics of laminar, transitional and turbulent flow in microchannels. The experimental data in some studies were found to contradict the conventional macroscale theory; see for example Mala and Li (1999), Sobhan and Garimella (2001), Obot (2002), Yang et al. (2003), Hsieh et al. (2004), Lee et al. (2005), Liu et al. (2007) and Tullius et al. (2011). Despite this discrepancy, some other studies did not find any size effect on fluid flow and heat transfer in microchannels; see for example Harms et al. (1999), Agostini et al. (2002), Judy et al. (2002), Li and Cui (2003), Lelea et al. (2004), Owahib and Palm (2004), Hwang and Kim (2006), Li et al. (2007), Hrnjak and Tu (2007), Hao et al. (2007) and Lin and Yang (2007). The discrepancies reported in the past studies can

be due to measurement uncertainties and scaling effects as reported by Rosa et al. (2009). They concluded that macro scale theory and correlations are valid at micro scale if measurement uncertainty and scaling effects were carefully considered. These scaling effects include: entrance effects, viscous heating, conjugate heat transfer, electric double layer effects, surface roughness, and properties dependent on temperature, compressibility and rarefactions (for gas flow only). The main aim of the past experimental studies was to verify whether the conventional theory is applicable at micro scale or new theories need to be developed to describe flow in microchannels as reported by Lee at al. (2005).

Performing experiments with microchannels can be very costly in both time and money. To reduce the number of experiments that need to be performed researchers employ Computational Fluid Dynamics (CFD) as a tool for heat transfer analysis. CFD can be used in parallel with experimental setups in an effort to predict the flow and heat transfer characteristics of given surface modification under the specified control parameters and boundary conditions. Computational methods can shorten the design cycle and thereby reduce experimental costs. Fedorov and Viskanta (2000) conducted 3D numerical simulations to investigate heat transfer in a rectangular microchannel with a range of hydraulic diameter D_h =10 – 100 μm and 10 mm channel length. They showed that the 3D simulation is capable of resolving the complex heat flux pattern due to the strong coupling between convection and conduction. Lee et al. (2005) performed a numerical simulation to solve a 3D conjugate heat transfer problem in a microchannel heat sink using a simplified thin-wall model. Five microchannels of different sizes D_h =318 – 903 μm and 25.4 mm length were investigated over a range of Reynolds number 300 - 3500. The numerical results were found to be in good agreement with experiments showing that the simplified thin wall analysis can be used to numerically analyze conjugate heat transfer.

Recently, Mansoor et al. (2012) performed 3D simulations for flow in a rectangular microchannel incorporating both conduction in the copper substrate and convection by the channel fluid. The microchannel had dimension of 194 μm, 884 μm, 25.4 mm for width, height, and length respectively. The simulations were carried out using the Fluent CFD code. The numerical results were compared with experimental and numerical results of Lee et al. (2005) and were found to be in a good agreement. They found that the average Nusselt number increased with increasing heat flux. They proposed a correlation for the average Nusselt number as given by Eq. (1), which is valid for *Re* = 500-2000.

$$Nu_{av} = 0.2931 \mathrm{Re}^{0.53} \mathrm{Pr}^{-0.25} \qquad (1)$$

The work presented herein this paper is a part of a main project on investigating experimentally and numerically single phase and flow boiling of de-ionized water in a rectangular microchannel. The aim of this paper is to validate the experimental thermal boundary conditions under single phase flow conditions using three different simulation schemes. Understanding the thermal boundary conditions is important before conducting two phase flow boiling simulations to make sure which simulation scheme is matching the experiments. Accordingly, the focus in the present numerical work is to examine the accuracy of different numerical schemes (2D versus 3D) through comparing the predicted friction factor and Nusselt number with experimental data and conventional theory.

2. Experimental Setup

The detailed description of the experimental facility was given by Mirmanto et al. (2012). It consists of reservoir, sub-cooler, gear pump with a programmable variable speed drive, coriolis flow meter, pre-heater, test section, inline filters and condenser as depicted in Fig. 1. A water-glycol circulation chiller is used for cooling duties in

the condenser and sub-cooler. De-ionized water was used as a test fluid. After de-gassing in the reservoir, water was circulated through the system and its temperature was controlled at the test section inlet through a PID controller. The test section was made of an oxygen-free copper block (12 mm wide x 25 mm high x 72 mm long). A single rectangular microchannel 0.39 mm high, 1 mm wide and 62 mm long was cut in the top surface of the block using a Kern HSPC 2216 high-speed micro-milling machine. The measurements were accurate to ± 2 μm giving a mean uncertainty of ±0.34% for the hydraulic diameter, 0.56 mm. The average surface roughness Ra of the channel base was measured using a Zygo NewView 5000 surface profiler with an accuracy of ±1 nm. The Ra value was found to be 0.392 μm near inlet, 0.242 μm near middle and 0.330 μm near outlet

The test section was heated using one cartridge heater embedded below and parallel to the channel length. Water inlet and outlet temperature was measured using K-type thermocouples while the axial channel bottom surface temperature was measured using six K-type thermocouples located 1.5 mm below the channel bottom. Six differential pressure sensors Honeywell 26PCC were used to measure the local pressure between channel inlet and outlet. All data were recorded using NI-compact modular data acquisition system with Labview software.

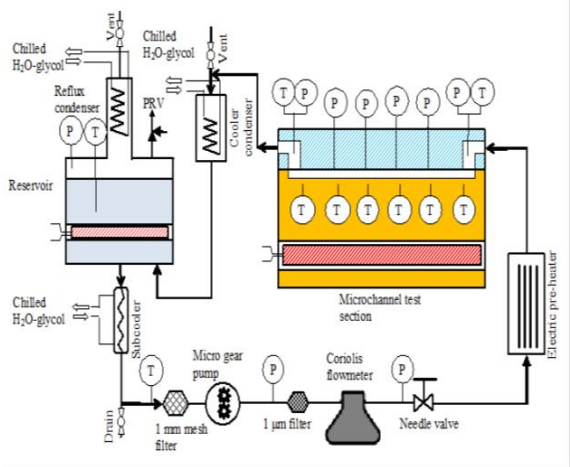

Fig. 1. Schematic of experimental facility, Mirmanto et al. (2012).

The pressure drop along the microchannel is given as:

$$\Delta p_{ch} = \Delta p_{meas} - \Delta p_{loss} \tag{2}$$

where ΔP_{loss} defined by Eq. (3) is the pressure loss due to the inlet and outlet manifolds and the sudden contraction and enlargement. The flow enters and leaves the channel in a direction normal to the flow direction.

$$\Delta p_{loss} = 2\left(\frac{1}{2}\rho V_p{}^2 K_{90}\right) + \frac{1}{2}\rho V_{ch}{}^2\left(K_c + K_e\right) \tag{3}$$

The Fanning friction factor was calculated using equation (4) as:

$$f = \frac{\Delta p_{ch} D_h}{2 L_{ch} \rho V_{ch}{}^2} \tag{4}$$

The rate of heat loss from the test section to the ambient was determined experimentally using an energy balance with the water flowing and was found to be approximately 7.23 % of the input electrical power at the cartridge heater. The rate of heat removal, q_{rem}, by the working fluid is given as:

$$q_{rem} = P - q_{loss} = \dot{m} c_p (T_o - T_i) \tag{5}$$

where P is equal to product of the voltage (V) and the current (I) supplied to the cartridge heater. An average heat flux is then calculated by applying equation (6):

$$q'' = \frac{q_{rem}}{A_{ht}} \tag{6}$$

The average heat transfer coefficient is given by:

$$h_{av} = \frac{q''}{\Delta T_{lm}} \tag{7}$$

$$\Delta T_{lm} = \frac{T_o - T_i}{\ln\left(\frac{(T_w - T_i)}{(T_w - T_o)}\right)} \tag{8}$$

The corresponding average Nusselt number is then calculated as:

$$\mathrm{Nu}_{\mathrm{av}} = \frac{h_{av} D_h}{k_f} \tag{9}$$

The propagated uncertainty in the measured friction factor and heat transfer coefficient was calculated according to the method described in Coleman and Steel (1999) and the average values were 10.2% and 6.3 % respectively.

3. Numerical Analysis

3.1 Description of models

The numerical simulations were performed to solve the conjugate heat transfer problem in a microchannel, accounting for both convection in the channel and conduction in the copper substrate. Four approaches were used:

1. 2D model: this model is shown in Fig. 2 where the inlet and outlet plenums are included and constant heat flux boundary condition is applied at the bottom surface.
2. 3D thin wall model (1 side heated): in this model, the wall thickness is zero and constant heat flux boundary condition was applied at the bottom surface only while other walls were considered adiabatic; see Fig. 3.
3. 3D thin wall model (3 sides heated): this model is similar to the one presented in Fig. 3 except that constant heat flux was applied at the bottom and two side walls while the top wall was kept adiabatic.
4. 3D full conjugated model: in this model, the full copper block, which is similar to the experiment, was simulated as seen in Fig. 4. A constant heat flux boundary condition was applied at the location of the cartridge heater. The inlet and outlet plenums are not included in this model.

The computations were performed using the commercial software package FLUENT 14.5. ICEM 14.5 was utilized for the geometry construction and mesh generation. The hexa meshing grid scheme was used to mesh the system. A highly compressed non-uniform grid near the channel walls was adopted in order to properly resolve viscous shear layers as seen in Fig. 5. Grid nodes were also concentrated along the axial direction in the entrance of the channel in order to properly resolve the flow and thermal development regions as adopted by Fedorov and Viskanta (2000) and Qu and Mudawar (2002).

3.2 Numerical method

A CFD analysis was carried out to investigate the characteristics of fluid flow and conjugate heat transfer in a microchannel. The following assumptions were adopted:

1. steady state fluid flow and heat transfer;
2. incompressible fluid;
3. negligible radiative heat transfer;
4. constant solid and fluid properties

Based on the above assumptions, the governing differential equations used to describe the fluid flow and heat transfer in the microchannel are given as:

Conservation of mass (continuity)

$$\nabla\left(\rho\vec{V}\right) = 0 \tag{10}$$

Conservation of momentum

$$\vec{V}\cdot\nabla\left(\rho\vec{V}\right) = -\nabla p + \nabla\cdot\left(\mu\nabla\vec{V}\right) \tag{11}$$

Conservation of energy for fluid

$$\vec{V}\cdot\nabla\left(\rho c_p T_f\right) = \nabla\cdot\left(k_f\nabla T_f\right) \tag{12}$$

Conservation of energy for solid

$$\nabla\cdot\left(k_w\nabla T_w\right) = 0 \tag{13}$$

A number of uniform inlet velocities were selected in order to match the Reynolds numbers obtained in the experiment. At the outlet a pressure outflow boundary condition was employed. The no slip boundary condition was assigned for all wall boundaries. The heat loss through the top over was considered to be negligible. In the thin wall approach adiabatic conditions were employed at the top wall while along the bottom (and also the side walls

for the 3D simulation) a constant heat flux, q'' was applied. Water temperature at the channel inlet was kept fixed at 35 ^{0}C. For the 3D fully conjugate analysis, the continuity of the temperature and heat flux is used as the conjugate boundary condition to couple the energy equations at the fluid and solid interface.

The viscous laminar model or standard k-Omega model was used for laminar ($Re < 2000$) and turbulent ($Re > 2200$) flow, respectively. The SIMPLE scheme is used to resolve the pressure-velocity coupling. The flow momentum and energy equations are solved with a first-order upwind scheme. The simulations are performed using a convergence criterion of 10^{-6}. A grid dependency study was conducted for friction factor at Re=205 to ensure the results are independent of the mesh. It was carried out in 3D model (thin wall model) by varying the number of grids in the microchannel. Three different grid sizes of $20 \times 50 \times 600$, $20 \times 15 \times 600$, and $20 \times 15 \times 300$ were used. Since no appreciable change in the value of friction factor was observed, the grid size of $20 \times 15 \times 300$ was chosen. The geometrical parameters used in the simulation are summarized in Table 1.

Fig.2. 2D Computational model

Table 1 Geometric parameters used for the thin-wall analysis.

Parameter	Value (mm)
Width of channel, W_{ch}	1
Height of channel, H_{ch}	0.39
Height of manifold, H_m	0.39
Height of plenum, H_p	8
Length of channel L_{ch}	62
Diameter of plenum, D_p	2
Diameter of manifold, D_m	2
Hydraulic diameter, D_h	0.561

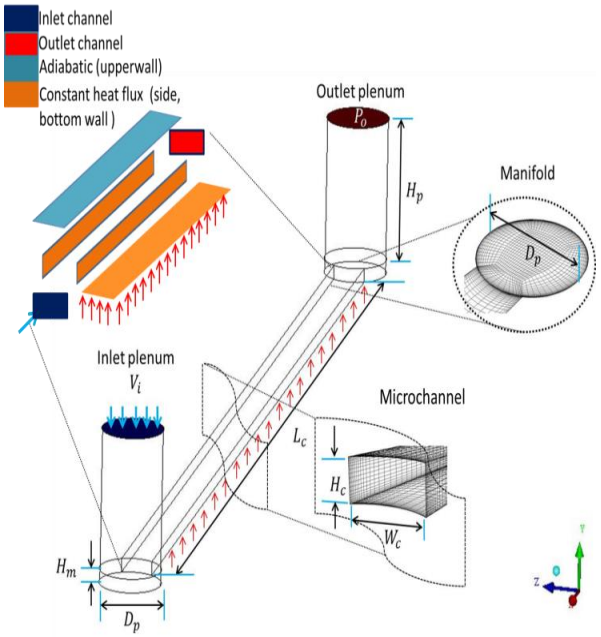

Fig. 3. 3D Computational domain thin-wall analysis (bottom side heated)

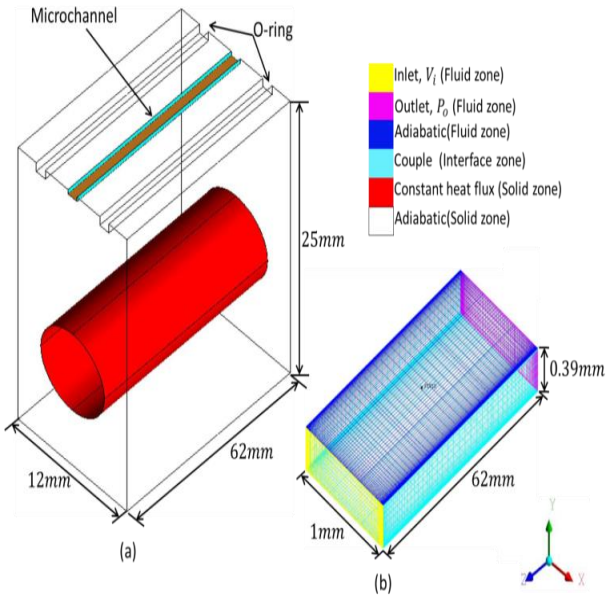

Fig. 4. Fully conjugate computational model (a) solid zone (b) fluid zone

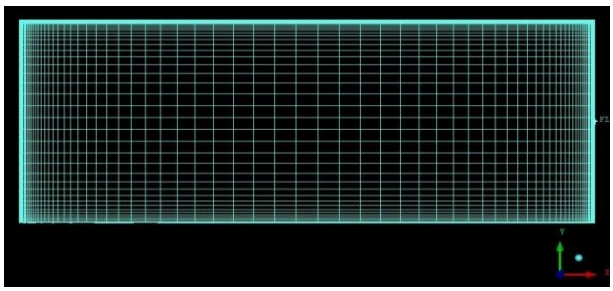

Fig. 5. Mesh generation (Fluid Zone)

3.3 Data analysis

The Reynolds number is defined as:

$$Re = \frac{\rho_f V D_h}{\mu_f} \quad (14)$$

The hydraulic diameter is defined as:

$$D_h = \frac{4W_{ch}H_{ch}}{2(W_{ch}+H_{hc})} \quad (15)$$

The Fanning friction factor is defined as:

$$f = \frac{\Delta P_{ch} D_h}{2L_{ch}\rho_f V^2} \quad (16)$$

and $\Delta P_{ch} = P_{inlet} - P_{outlet}$

The local heat transfer coefficient is defined as:

$$h(x) = \frac{q''(x)}{T_{w,av} - T_{f,av}} \quad (17)$$

These temperatures were the average of five locations along the channel width at each axial distance. The local Nusselt number is defined as:

$$Nu(x) = \frac{h(x)D_h}{k_f} \quad (18)$$

The average heat transfer coefficient is defined as:

$$h_{av} = \frac{1}{L}\int_0^L h(x)dx \quad (19)$$

and the average Nusselt number is defined as:

$$Nu_{av} = \frac{h_{av}D_h}{k_f} \quad (20)$$

4. Results and Discussions

The numerical results were verified using experimental data and the Shah and London (1978) correlations for developed and developing laminar flow and Blasius (1913) equation for turbulent flow as seen in Figs. 6 and 7. Figure 6 depicts the validation of the friction factor predicted by the 2D and 3D models. The figure indicates that the 2D model underpredicts the values by about 30% while the 3D model agrees very well with the experimental data. Additionally, it is obvious that both 3D model and experimental data exhibit a small transition jump at Re ≈ 1600. In other words, the early transition reported by some researchers (Re < 1000) was not observed in the present study, which agrees with Harms et al. (1999) and Zhang et al. (2014). Harms et al. (1999) investigated water flow in rectangular microchannel ($D_h = 401\ \mu m$) and found that the transition occurrs at $Re \approx 1500$. Recently, Zhang, et al. (2014) studied flow and heat transfer characteristics of six rectangular microchannels with D_h ranging from $0.48\ mm$ to $0.84\ mm$. The experimental results show that the laminar to turbulent transition occurs at $Re = 1200 - 1600$. Researchers who reported early transition believed that it occurs due to channel size reduction as reported by Peng et al. (1995) and Pfund et al. (2000).

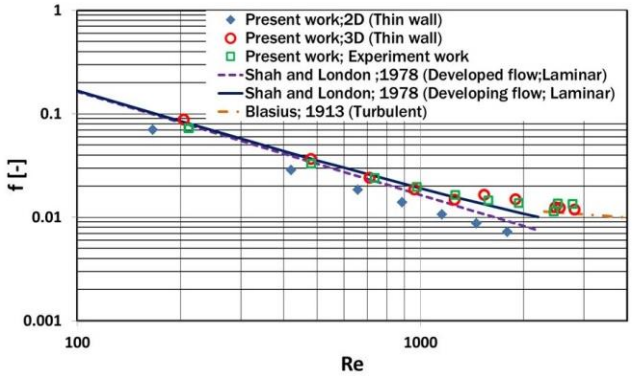

Fig. 6. Comparison of predicted friction factor with existing experimental results and correlation

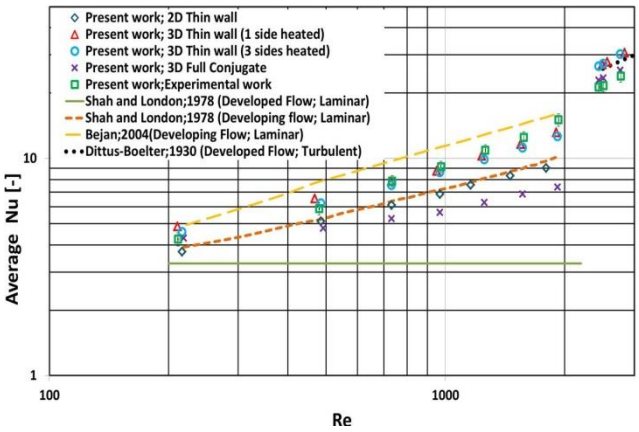

Fig. 7. Comparison of predicted average Nusselt number with experimental data and correlations

Figure 7 presents a comparison of the computationally predicted average Nusselt number in the laminar and turbulent regions with experimental data and correlations. The figure shows that the 2D thin wall model agrees very well with Shah and London (1978) for developing laminar flow but highly under-predicts the experimental values. This could be due to the fact that Shah and London solved the 2D problem. The 3D thin-wall models (one side and three side heated) exhibit excellent agreement with the experimental values. In these models, the wall heat flux was assumed constant and the insignificant difference between the two models could be due to the short height of the channel ($0.39\,mm$). On contrast, the 3D full conjugate model (simulating the experiment) highly under-predicts the experimental values particulary when Reynolds number increases in the laminar region. This deviation may be attributed to two reasons. The first reason could be due to the fact that the inlet and outlet manifolds are not included in this model while they are included in the other thin-wall models. It means that the enhancement in heat transfer induced by turbulence at the inlet is not included. This may explain the agreement between all models at the lowest Reynolds number, i.e. turbulence due to inlet manifold is weak. The second possible reason could be due to the conjugate effect, i.e. heat flux is not uniformly distributed along the channel. To clarify this point, the local heat flux along the channel was plotted in Fig. 8 for the bottom and side walls. The local heat flux is defined as $q'' = k_f \Delta T / \Delta y$. The figure demonstrates that the heat flux is very high near the entry region due to the thin thermal boundary layer and then it decreases contineously along the channel. Thus, the average Nusselt number is expected to be lower than the thin-wall models in which the heat flux is assumed constant. The high heat flux in the entry region was also found by Qu and Mudawar (2002) and Tiselj et al. (2004). As illustrated in Fig. 8, the heat flux varies in the cross-stream direction where the heat flux at the bottom wall was found to be higher compared to that at the side walls. This is due to the fact the near-wall flow velocity in the middle of the bottom wall is larger than in the middle of the (smaller) side walls. A higher near-wall velocity results in an increased (wall-averaged) heat transfer rate. It is interesting to note that the experimental results in Fig. 7 agrees with the thin-wall models although the conjugate model is simulating the experiment. This may be attributed to the assumption of constant wall heat flux adopted in the experimental data reduction. This means that the effect of conjugate heat should be taken into consideration as also reported by Iaccarinno et al. (2002).

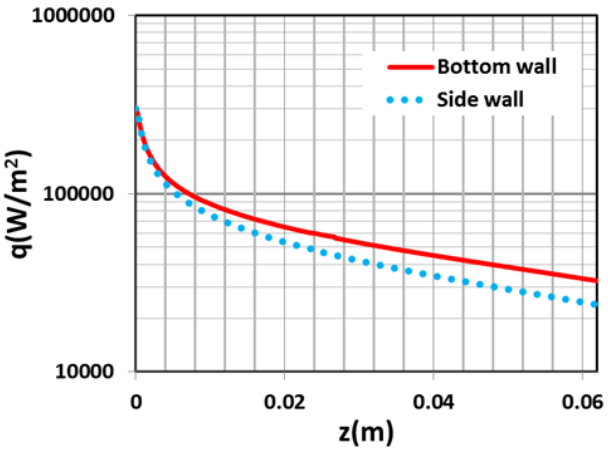

Fig. 8. Local heat flux distribution for bottom and side wall along the channel length

Figure 9 depicts the fluid and channel bottom wall temperature along the channel length for the 3D thin-wall approach three side heated (Fig. 9a) and the 3D conjugate heat transfer approach (Fig. 9b) at Re = 216. It is worth mentioning that in the thin wall approach uniform heat flux (at the bottom and side walls) boundary condition was assumed. In the full conjugate heat transfer approach, the full cooper block with the embeded cartridge heater was simulated, which is exactly the same as the experiment. As seen in Fig. 9a, as expected from the theory for constant heat flux boundary condition, the fluid and wall temperature increase linearly in the fully developed region. This trend is expected to occur because the wall thickness was assumed to be zero, i.e. there is no conjugate effect. On the contrary, Fig. 9b demonstrates a very clear conjugate effect

where the wall and fluid temperatures are not linear although constant heat flux boundary condition was assumed at the location of the cartridge heater, see Fig. 3. The high thermal conductivity of copper makes the heat transfer problem multi-dimension and consequently the wall temperature approaches from the isothermal conditions. The wall temperature measured at six axial locations is also included in Fig. 9b. The measured values were corrected using 1D heat conduction to consider the 1.5 mm distance between the thermocouple and channel base. As seen in the figure, the simulation predicts exactly similar trend to the experiment but slightly higher values.

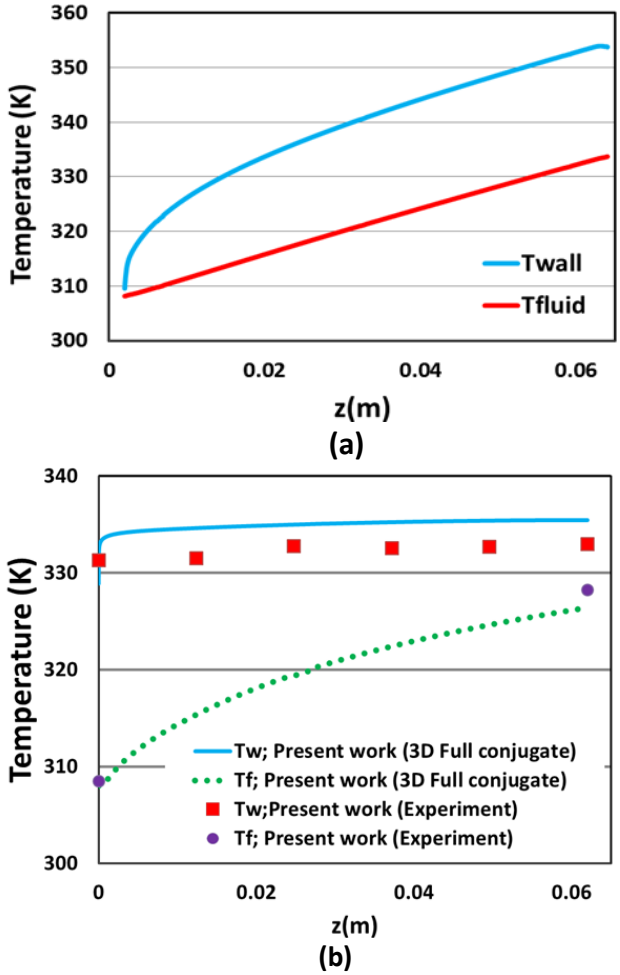

Fig. 9. Axial temperature variation of fluid and bottom wall along the channel at Re=216 a) Thin wall analysis, 3 side heated b) Full conjugate analysis

Figure 10 presents the local Nusselt number versus axial distance for the four models at Re = 216. It is clearly shown that *Nu* predicted by the 2D and 3D thin-wall models approaches a fully developed constant value of 2.37 and 3.34 respectively. On the contrary, the *Nu* predicted by the 3D full conjugate model decreases continously with axial distance. This confirms that the boundary condition at the channel walls is not constant heat flux as previously discussed in Fig. 8. Comparing the 2D and 3D thin wall simulation results in Fig. 6 and 7, it can be seen that the predicted friction factor and local Nusselt number in the 2D simulation are lower than in the 3D simulation. This is due to the presnce of side-walls in the 3D simulation that give rise to cross-stream fluid motions resulting in higher values for both *f* and *Nu*.

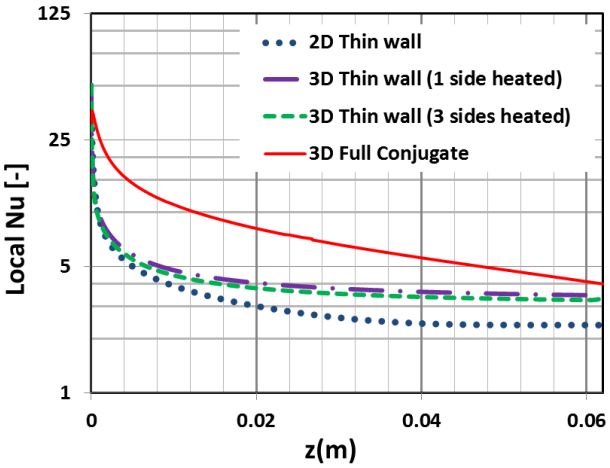

Fig. 10.below Variation of local Nusselt number along the channel

The numerical results found in this study agree with the findings of Moharana et al. (2012). They conducted a numerical study on simultaneously developing flow under conjugate conditions in a square microchannel. They studied the effect of substrate thickness and thermal conductivity on heat transfer characteristics. They found that, the local heat flux becomes uniformly distributed along the channel after the entry region when the substrate thickness becomes very small (thin wall approach in the present study) or when the substrate thermal conductivity becomes very low. In this case, they found that the wall and fluid temperatures are linear as found in the current study, see Fig. 9a. When the substrate thickness and thermal conductivity was high (full conjugate model in the present

study), the heat flux was found to decrease with axial distance, see Fig. 10.

5. Conclusions

A numerical study has been carried out to investigate single phase heat transfer and fluid flow in a rectangular microchannel using water as a working fluid. Four models were investigated namely 2D, 3D thin-wall (one side heated), 3D thin-wall (three side heated) and 3D fully conjugate heat transfer model. The simulation was conducted using FLUENT 14.5. The main conclusions are summarized as follows:

1. The experimental and numerical results demonstrated that transition from laminar to turbulent occurs at Re = 1600 – 2000.
2. The 3D thin-wall models predicted the experimental values with excellent agreement compared to the 3D conjugate model. The deviation between the experimental values and conjugate model could be due to the fact that conjugate effects are not taken into consideration in the experimental data reduction process.

Nomenclature

A_{ht}	heat transfer area $A_{ht} = (W_{ch} + 2H_{ch})L$, [m^2]
c_p	specific heat, [J/kg K]
D	diameter, [m]
D_h	hydraulic diameter, [m]
f	Fanning friction factor [-]
H	height, [m]
h	heat transfer coefficient, [W/m^{2}K]
I	current, [A]
K_{90}	pressure loss coefficient, [-]
K_c	sudden contraction coefficient, [-]
K_e	sudden enlargement coefficient, [-]
k	thermal conductivity, [W/m K]
L	length, [m]
$\dot{m}$	mass flow rate, [kg/s]
Nu	Nusselt, [-]
Pr	Prandtl, [-]
P	pressure, [Pa] or Power, [w]
ΔP	pressure difference, [Pa]
q	heat rate, [W]
q''	heat flux, [W/ m^2]
Re	Reynolds number, [-]
T	temperature [K]
ΔT	temperature difference, [K]
ΔT_{lm}	log-mean temperature difference, [K]
V	voltage, [V] or velocity, [m/s]
W	width, [m]
x	axial distance, [m]
Δy	vertical distance, [m]

Greek symbols

μ	viscosity, [kg/m s]
ρ	density, [kg/m^3]

Subscripts

av	average
ch	channel
f	fluid
i	in
m	manifold
meas	measured
o	out
p	plenum
rem	net removal
w	wall
w, av	average wall

References

Agostini, B., Watel, B., Bontemps, A., and Thonon, B. 2002. Friction factor and heat transfer coefficient of R-134a liquid flow in minichannels. Applied Thermal Engineering, 22,1821–1834.

Bejan, A., 2004. Convection Heat Transfer. New Jersey: John Wiley and Son, Inc.

Blasius, H. Das 1913. Ähnlichkeitsgesetz bei Reibungsvorgängen in Flüssigkeiten, Forchg. Arb. Ing.-Wes., No. 131, Berlin.

Celata, G. P., Cumo, M., Gugliemi, M. and Zummo, G., 2002. Experimental Investigation in Hydraulic and Single-Phase Heat Transfer in 0.130mm Capillary Tube. Microscale Thermphysical Engineering, Volume 6, 85-97.

Coleman, H. W. and W.G. Steele. 1999. Experimentation and uncertainty analysis for engineers, John Wiley and Sons Inc. Second edition, New York.

Choi, S., Barron, R. and Warrington , R., 1991.

Fluid flow and heat transfer in microtubes. Micromechanical Sensors, Actuators, and Systems, ASME, Volume 32, 123-133.

Fedorov, A. G. and Viskanta, R., 2000. Three-dimensional Conjugate Heat Transfer in The Microchannel Heat Sink for Electronic Packaging. International Journal of Heat and Mass Transfer , Volume 43, 399-415.

Hao, P-F., Zhang, X-W., Yao, Z-H. and He F. 2007. Transitional and turbulent flow in a circular microtube. Experimental Thermal and Fluid science, 32: 423 – 431.

Harms, T. M., Kazmierczak, M. J. and Gerner, F. M., 1999. Developing Convective Heat Transfer in Deep Rectangular Microchannels. International Journal of Heat and Fluid Flow, Volume 20, 149-157.

Hrnjak, P. and Tu, X. 2007. Single phase pressure drop in microchannels. Int. J. Heat Fluid Flow, 28:2 – 14,

Hsieh, S-S., Lin, C-Y. and Huang, C-F. 2004. Liquid flow in a micro-channel. J. of Micomechanics and Microengineering, 14, 436–445.

Hwang, Y. W. and Kim, M. S. 2006. The pressure drop in microtubes and the correlation development. Int. J. Heat Mass Transfer, 49:1804 – 1812.

Iaccarinno , G., Ooi, A., Durbin, P. and Behnia, M., 2002. Conjugate heat transfer predictions in two-dimensional ribbed passages. International Journal of Heat and Fluid Flow, Volume 23, 340-345.

Judy, J., Maynes, D. and Webb, B., 2002. Characterization of frictional pressure drop for liquid flows through microchannels. International Journal of Heat and Mass Transfer , Volume 45, 3477-3489.

Lee, P.-S., Suresh, G. V. and Liu, D., 2005. Investigation of heat trasnfr in rectangular microchannels. International Journal of Heat and Mass Transfer, Volume 45, 1688-1704.

Lelea, D., Nishio, S. and Takano, K. 2004. The experimental research on microtube heat transfer and fluid flow of distilled water. Int. J. Heat Mass Transfer, 47: 2817 – 2830.

Li, Z-H., and Cui, H-H. 2003. Experiments about simple liquid flows in microtubes. 1st International Conference on Microchannels and Mininchannels, April 21 – 23, Rochester, New York, USA.

Li, Z., He, Y-L, Tang, G-H and Tao, W-Q. 2007. Experimental and numerical studies of liquid flow and heat transfer in microtubes. Int. J. Heat Mass Transfer, 50: 3447–3460.

Lin, T-W. and Yang, C-Y. 2007. An experimental investigation on forced convection heat transfer performance in microtubes by the method of liquid crystal thermography. Int. J. Heat Mass Transfer, 50, 4736 – 4742.

Liu, Z., Zhang, C., Huo, Y., and Zhao, X. 2007. Flow and heat transfer in rough micro steel tubes. Experimental Heat Transfer, 20: 289 – 306.

Mala, G. M. and Li, D. 1999. Flow characteristics of water in micro tubes. Int. J. Heat and Fluid Flow, 20 (2): 142– 148.

Mansoor, M. M., Wong, K.-C. and Siddique, M., 2012. Numerical investigation of fluid flow and heat transfer under high heat flux using rectangular micro-channels.. International Communications in Heat and Mass Transfer, Volume 39, 291-297.

Mirmanto, Kenning, D. B. R., Karayiannis, T. G. and Lewis, J. S., 2012. Pressure drop and heat transfer characteristics for single phase developing flow of water in rectangular microchannels. J. of Physics: Conference Series 395:012085.

Moharana, M. K., Singh, P. K., and Khandekar, S. 2012. Optimum Nusslet Number for Simultaneously Developing Internal Flow Under Conjugate Conditions in a Square Microchannel. J. Heat Transfer, 134, 1-10.

Obot, N., 2002. Toward A Better Understanding of Frivtion and Heat/ Mass Transfer in Microchannels. Microscale Thermophysical Engineeering , Volume 6, 155-173.

Owhaib, W. and Palm, B., 2004. Experimental investigation of single phase convective heat transfer in circular microchannels.. Experimetal Thermal and Fluid Science , Volume 28, 105-110.

Peng, X. and Peterson, G., 1996. Convection heat transfer and flow friction for water flow in microchannel structures. Int. J. Heat Mass Transfer, 39(12), 2599-2608.

Peng, X., Peterson, G. and Wang, B., 1995. Frictional flow characteristics of water flowing through rectangular microchannels. Experimental Heat Transfer, 249-264.

Pfund, D. et al., 2000. Pressure drop Measurements in Microchannel. AIChE Journal, 46(8), 1496-1507.

Qu, W. and Mudawar, I., 2002. Experimental and Numerical Study of Pressure Drop and Heat Transfer in A Single-Phase Microchannel Heat Sink. International Journal of Heat and Mass Transfer , Volume 45, 2549-2565.

Rosa, P., Karayiannis , T. and Collins, M., 2009.

Single-phase Heat Transfer in Microchannels: The Important of Scalling Effects. Applied Thermal Engineering , Volume 29, 3447-3468.

Shah, R.K. and London, A. L. (1978). Laminar flow forced convection in ducts. In: Irvin TF, Hartnett JP (eds) Advances in Heat Transfer. Academic , New York, 51 – 52, 124 – 128.

Sobhan, C. B. and Garimella, S. V., 2001. A Comparative Analysis of Studies on Heat Trasnfer and Fluid Flow in Microchannels. Microscale Thermophysical Engineering , Volume 5, 293-311.

Tiselj, I., Hetsroni G., Mavko, B. Mosyak A., Pogrebnyak E., and Segal Z., 2004. Effect of Axial Conduction on The Heat Transfer in Microchannels.. International Journal of Heat and Mass Transfer, Volume 47, 2551-2565.

Tuckerman, D. and Pease, R., 1981. High-performance heat sinking for VLSI. *IEEE* Electron Device Letters, Volume 5, 126-129.

Tullius, J. F., Vajtai, R. and Bayazitoglu, Y., 2011. A Review of Cooling in Microchannels. Heat Transfer Engineering, 32(7-8), 527-541.

Wang, B. and Peng, X., 1994. Experimental investigation on liquid forced convection heat transfer through microchannels,. International Journal Heat Mass Transfer , Volume 37, 73-82.

Yang, C-Y., Wu, J-C., Chien, H-T., and Lu, S-R. 2003. Friction characteristics of water, R134a and air in small tubes. Microscale Thermophysical Engineering, 7:335–348.

Zhang, J., Diao, Y., Zhao, Y. and Zhang, Y., 2014. An experimental study of the characteristics of fluid flow and heat transfer in the multiport microchannel flat tube. Applied Thermal Engineering, Volume 65, 209-218.